

A report on how infection of an RBC by the malarial parasite, *Plasmodium falciparum* affects the optical trapping characteristics and induces extraordinarily large torques that result in rotational motion of the trapped, infected cell has been published recently<sup>25</sup>.

1. Ashkin, A., Dziedzic, J. M., Bjorkholm, J. E. and Chu, S., Observation of a single-beam gradient force optical trap for dielectric particles. *Opt. Lett.*, 1986, **11**, 288–290.
2. Schutze, K., Posl, G. and Lahr, G., Laser micromanipulation systems as universal tools in cellular and molecular biology and in medicine. *Cell. Mol. Biol.*, 1998, **44**, 735–746.
3. Zahn, M. and Seeger, S., Optical tweezers in pharmacology. *Cell. Mol. Biol.*, 1998, **44**, 747–761.
4. Clement-Sengewald, A., Schutze, K., Ashkin, A., Palma, G. A., Kerlen, G. and Brem, G., Fertilization of bovine oocytes induced solely with combined laser microbeam and optical tweezers. *J. Assisted Reprod. Genet.*, 1996, **13**, 259–265.
5. Zahn, M., Renken, J. and Seeger, S., Fluorimetric multiparameter cell assay at the single cell level fabricated by optical tweezers. *FEBS Lett.*, 1999, **443**, 337–340.
6. Bustamante, C., Bryant, Z. and Smith, S. B., Ten years of tension: single-molecule DNA mechanics. *Nature*, 2003, **421**, 423–427.
7. Krantz, A., Red-cell mediated therapy: opportunities and challenges. *Blood Cells, Mol. Dis.*, 1997, **23**, 58–68.
8. Sato, S., Ishigure, M. and Inaba, H., Optical trapping and rotational manipulation of microscopic particles and biological cells using higher-order mode Nd-YAG laser beams. *Electr. Lett.*, 1991, **27**, 1831–1832.
9. Guck, J., Ananthakrishnan, R., Mahmood, H., Moon, T. J., Cunningham, C. C. and Kas, J., The optical stretcher: A novel laser tool to micromanipulate cells. *Biophys. J.*, 2001, **81**, 767–784.
10. Gaithier, R. C., Theoretical investigation of the optical trapping force and torque on cylindrical micro-objects. *J. Opt. Soc. Am. B*, 1997, **14**, 3323–3333.
11. Gaithier, R. C., Ashman, M. and Grover, C. P., Experimental confirmation of the optical-trapping properties of cylindrical objects. *Appl. Opt.*, 1999, **38**, 4861–4869.
12. Bar-Ziv, R., Meller, A., Tlusty, T., Moses, E., Stavans, J. and Safran, S. A., Localized dynamic light scattering: Probing single particle dynamics at the nanoscale. *Phys. Rev. Lett.*, 1997, **78**, 154–157.
13. Meller, A., Bar-Ziv, R., Tlusty, T., Moses, E., Stavans, J. and Safran, S. A., Localized dynamic light scattering: A new approach to dynamic measurements in optical microscopy. *Biophys. J.*, 1998, **74**, 1541–1548.
14. Elgsaeter, A., Stokke, B. T., Mikkelsen, A. and Branton, D., The molecular basis of erythrocyte shape. *Science*, 1986, **234**, 1217–1223.
15. Neuman, K. C., Chadd, E. H., Liou, G. F., Bergman, K. and Block, S. M., Characterization of photodamage to *Escherichia coli* in optical traps. *Biophys. J.*, 1999, **77**, 2856–2863.
16. Ashkin, A., Schuetze, K., Dziedzic, J. M., Euteneuer, U. and Schliwa, M., Force generation of organelle transport measured *in vivo* by an infrared laser trap. *Nature*, 1990, **348**, 346–348.
17. Block, S. M., Blair, D. F. and Berg, H. C., Compliance of bacterial flagella measured with optical tweezers. *Nature*, 1989, **338**, 514–518.
18. Svoboda, K. and Block, S. M., Biological applications of optical forces. *Annu. Rev. Biophys. Biomol. Struct.*, 1994, **23**, 247–285.
19. Mukhopadhyay, R., Lim, G. H. W. and Wortis, M., Echinocyte shapes: bending, stretching, and shear determine spicule shape and spacing. *Biophys. J.*, 2002, **82**, 1756–1772.
20. Landau, L. D. and Lifshitz, E. M., *Theory of Elasticity*, Pergamon Press, New York, 1959, p. 56.
21. Henon, S., Lenormand, G., Richert, A. and Gallet, F., A new determination of the shear modulus of the human erythrocyte membrane using optical tweezers. *Biophys. J.*, 1999, **76**, 1145–1151.
22. Friese, M. E. J., Enger, J., Rubinsztein-Dunlop, H. and Heckenberg, R. N., Optical angular-momentum transfer to trapped absorbing particles. *Phys. Rev. A*, 1996, **54**, 1593–1596.
23. Simpson, N. B., Dholakia, K., Allen, N. and Padgett, M. J., Mechanical equivalent of the spin and orbital angular momentum of light: an optical spanner. *Opt. Lett.*, 1997, **22**, 52–54.
24. Cheng, Z., Chaikin, P. M. and Mason, T. G., Light streak tracking of optically trapped thin microdisks. *Phys. Rev. Lett.*, 2002, **89**, 108303 1–4.
25. Dharmadhikari, J. A., Roy, S., Dharmadhikari, A. K., Sharma, S., and Mathur, D., Torque-generating malaria-infected red blood cells. *Opt. Express*, 2004, **12**, 1179–1184.

ACKNOWLEDGEMENTS. We have benefited from many stimulating discussions with our colleagues, B. J. Rao and Sunil Noothi, which have helped us design and fabricate the optical trap to study the manipulation of single biomolecules. We are grateful to Shobhona Sharma and Sunando Roy for providing red blood cell samples used in these experiments. Useful discussions with them and with R. G. Pillay, M. Krishnamurthy and Amit Roy are acknowledged. We thank Sakti Narayan for initial measurements of some of the laser parameters.

Received 3 January 2004; accepted 7 April 2004

## A combined approach of Schlumberger and axial pole–dipole configurations for groundwater exploration in hard-rock areas

S. Chandra\*, V. Anand Rao and V. S. Singh

Groundwater Exploration and Management Group, National Geophysical Research Institute, Uppal Road, Hyderabad 500 007, India

**In hard rocks, groundwater accumulation occurs only because of secondary porosity developed due to weathering, fracturing, faulting, etc., which is highly variable and varies sharply within very short distances, contributing to near-surface inhomogeneity. This can affect the current-flow pattern in their surroundings and consequently distort the resistivity curve, and hence falsify the interpretation in terms of layer resistivity and its thickness. Thus it becomes a difficult task for locating a good well site in hard rocks. A combined approach of Schlumberger and axial pole–dipole configurations has been initiated, which will be helpful in locating the successful sites for drilling of wells in hard-rock areas. It is also suggested that the axial pole–dipole array can be applied for groundwater exploration even at places where Schlumberger**

\*For correspondence. (e-mail: chandra\_sngri@rediffmail.com)

**configuration could not be laid due to non-availability of space on any one side of the sounding location.**

**The aim of this communication is to demonstrate the detectability of near-surface inhomogeneity effect in the sounding curve by combined use of Schlumberger and axial pole-dipole configurations, with field examples carried out over the two different kinds of rock terrains, viz. Dharwar (Archean granitic) and Vindhyan (Precambrian sedimentary).**

IN groundwater studies, the resistivity method can furnish information on subsurface geology, which might be unattainable by other geophysical methods. For example, electrical methods are unique in furnishing information concerning the depth of the freshwater-saltwater interface, whereas neither gravity, magnetic nor seismic methods can supply such information. The apparent resistivity is generally measured using Wenner, Schlumberger, dipole-dipole electrode configurations, etc. Groundwater exploration in hard rocks is fraught with several difficulties on account of wide and erratic variation of vital parameters, which characterize the groundwater regime. Spatial variation of these characteristic parameters is attributed, among other causes, to tectonic activities and degree of weathering of near-surface rocks<sup>1</sup>. These processes induce, directly or indirectly, secondary porosity in the rocks to a variable extent. As a result, the groundwater potential also varies significantly from place to place even in the same geological formation.

In hard rock areas, at many places the lateral inhomogeneity, viz. sheet rocks, dykes, buried boulders, buried channel, etc. occurs close to the surface, which distorts the current flow pattern in their surroundings and consequently there is distortion in the resistivity curve. It has been observed in the field and also mentioned in the literature that when the current electrode (Schlumberger array) is in the vicinity of the lateral inhomogeneity, the slope of the resistivity curve changes abruptly compared to the trend obtained for earlier electrode spacing<sup>2-4</sup>. The effect of these lateral inhomogeneities on the resistivity curves depends on size and geometry of the inhomogeneity, resistivity contrast between inhomogeneity and surrounding media, type of electrode configuration used and angle of electrode spread with respect to the inhomogeneity<sup>5</sup>. The distortion in the VES curve results as false interpretation in terms of layer resistivity and its thickness/depth. Thus it became essential to identify and remove the effect of lateral inhomogeneity from VES curves before arriving at unambiguous interpretation and giving any recommendation for drilling the wells.

The Lee-partitioning electrode configuration, which is the modified configuration of Wenner array using one extra potential electrode at the centre of the configuration, has an advantage of measuring lateral changes in resistivity of the subsurface. The apparent resistivities were calculated for each half of the array<sup>6</sup>. Frohlich<sup>7</sup> has studied the influence of lateral inhomogeneities on the dipole

methods and compared it with the Schlumberger methods. It was found that the dipole method is more influenced by lateral inhomogeneities than the Schlumberger method. Ballukaraya *et al.*<sup>5</sup> have studied the identification of lateral inhomogeneities from VES curves in the laboratory with the help of a tank model as well as in the field. The tank was filled with uniformly graded soil having a resistivity of approximately 160 ohm m, with a vertically placed resistive body (glass plate,  $0.75 \times 0.50 \text{ m}^2$  size) across the electrode-spread direction slightly below the surface. They discussed three methodologies for identification of lateral inhomogeneities, i.e. offset sounding, radial sounding and magnitude of current.

The offset sounding method deals with ways to study a VES response for differentiating between horizontal and lateral inhomogeneities by carrying out two or more vertical electrical soundings close to each other (about 10 m) along a common azimuth. A sharp resistivity contrast due to lateral inhomogeneities on VES curves can be seen by an abrupt change in the curve slope. The half current electrode separation ( $a/2$ ) at which the change in the slope occurs in the various VES curves, is offset by the distance between the sounding stations. In the case of vertical discontinuity (sub-surface), the change in the slope occurs approximately at same point for all the VES curves provided the VES locations are not far-off from each other. While in the presence of lateral inhomogeneity, the slope in the VES curves is not at same point.

The radial sounding method deals with radial sounding carried out over the layered earth comprised of horizontal layers, which are isotropic and homogeneous and have identical curves (no change in the measured apparent resistivity values) obtained at a given station in different azimuths. But in the presence of lateral inhomogeneity, the curves obtained at a given station will be different for different azimuths because the distance from the sounding station to the lateral inhomogeneity will vary along with the change in the spread directions. Thus the lateral inhomogeneity can be located by carrying out radial sounding with different azimuths at a particular station.

The magnitude of current is another method used by Ballukaraiya *et al.*<sup>5</sup> for identification of lateral inhomogeneities, where a controlled current source is used for carrying out VES measurements. In the presence of lateral inhomogeneity, when a current electrode approaches towards it or is placed over it, the adjusted current magnitude drops down. Thus any sharp change in the slope of the VES curve at such electrode separation can be attributed to the presence of a lateral inhomogeneity.

Ermokhin *et al.*<sup>8</sup> have worked on the calculation of the azimuthal inhomogeneity ratio response of 3D structures using an analytical forward modelling scheme. The azimuthal inhomogeneity ratio can be obtained by measuring the three possible modes of connection for resistance measurements with the square array and it reflects the presence of subterranean lateral inhomogeneities.

The above-discussed methods of identification of lateral inhomogeneity are either more time-consuming, as they need two or more than two soundings, or are not convenient. Here it is demonstrated that the near-surface inhomogeneity effect can be clearly identified using combined electrode configuration, i.e. Schlumberger and axial pole-dipole. This combination requires less time as it is carried out on the same traverse simultaneously keeping one extra current electrode at infinity.

In order to identify the lateral inhomogeneities, a combined set-up of Schlumberger and axial pole-dipole arrays has been experimented. This combined set-up (Figure 1) requires three current and two potential electrodes, which are similar to the Schlumberger set-up with one additional current electrode at infinity. The electric current-flow pattern and equipotential lines over isotropic and homogeneous ground for Schlumberger and axial pole-dipole (AMN) configuration have been shown in Figure 2. The axial pole-dipole (BMN) array is the mirror image of the AMN array. The current-flow pattern and equipotential lines will be disturbed over the surface having lateral inhomogeneities. The apparent resistivity ( $r_a$ ) can be calculated for Schlumberger and axial pole-dipole configurations as

$$r_a = \pi \frac{(a/2)^2 - (b/2)^2}{b} \frac{\Delta V}{\dot{E}}, \quad (1)$$

$$r_a = 2\pi \frac{(a/2)^2 - (b/2)^2}{b} \frac{\Delta V}{\dot{E}}, \quad (2)$$

where  $a/2$  is the distance between the centre of the configuration and the outermost active current electrode,  $b/2$  is half of the potential electrode separation,  $I$  indicates injected current (in mA) into the ground and  $V$  denotes voltage difference between potential electrodes.

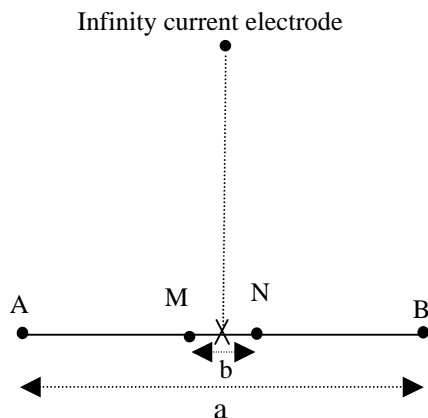


Figure 1. Combined set-up of Schlumberger and axial pole-dipole configurations.

The first reading is taken for Schlumberger array as usual by keeping the infinity current electrode disconnected. Next, one side of the current electrode (i.e. current electrode-B, Figure 1) of the Schlumberger array is replaced by the infinity current electrode to make it an axial pole-dipole set-up. This makes the reading for axial pole-dipole (AMN) array. Similarly, if current electrode-A of the Schlumberger array (refer to Figure 1) is replaced with the infinity current electrode, then the reading is for axial pole-dipole (MNB) array. The apparent resistivity values obtained from Schlumberger, i.e. AMNB and axial pole-dipole, i.e. AMN and MNB are plotted on log-log sheet and then compared with each other. If all curves are similar, the anomaly refers to the effect of sub-surface strata. In case these are dissimilar or showing anomaly at different  $a/2$ , the curve indicates the effect of near-surface inhomogeneity.

Geoelectrical soundings have been carried out in the hard-rock granitic terrain of Bairasagara watershed, Kolar district, Karnataka and in the Vindhyan (sedimentary) terrain at Mirzapur district, Uttar Pradesh (UP) using Schlumberger and axial pole-dipole configurations at

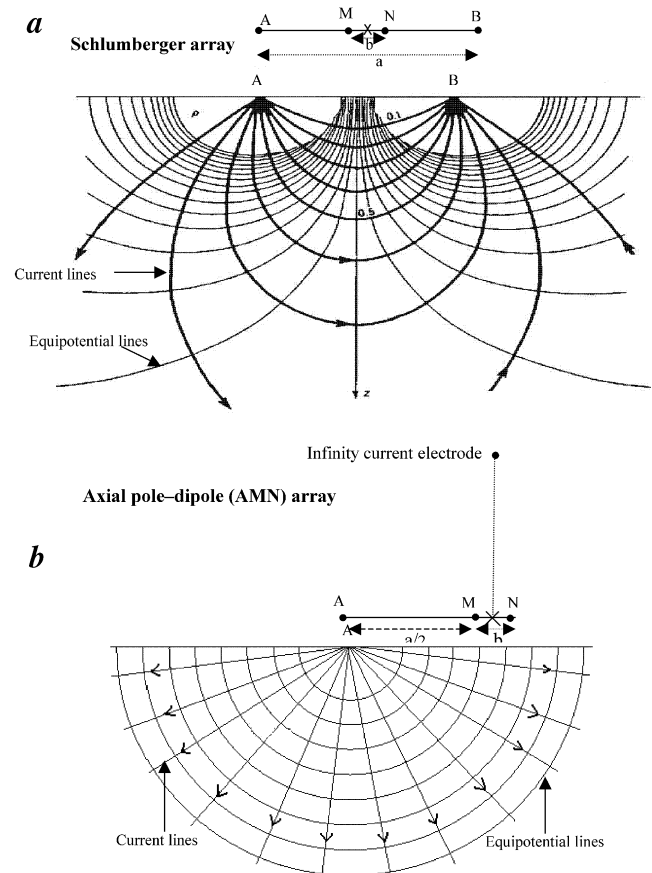


Figure 2. Schematic representation and current-flow pattern over homogeneous ground for (a) Schlumberger and (b) axial pole-dipole (AMN) configurations.

each location to detect the anomaly by comparing the interpreted results of both configurations. The granitic terrain at Bairasagara watershed belongs to the Dharwar super group of Archean age. The area has been traversed by a number of dolerite dykes trending in E–W direction. The rock formations have been weathered/fractured up to a depth of 46 m. The sedimentary terrain at Mirzapur belongs to the Kaimur Formation of the Vindhyan super group. The primary porosity in the rock is almost negligible and groundwater occurs in weathered/fractured zone of basement rocks in water table and semi-confined conditions<sup>9,10</sup>.

All the sounding data have been interpreted by conventional curve-matching technique<sup>11</sup> and using ‘GENRES’ software. The typical field examples of resistivity curves obtained by Schlumberger and axial pole–dipole configurations are shown in Figures 3–5. The sounding curves shown in Figure 3a and b have been carried out over granitic terrain of Bairasagara watershed and those shown in Figure 4a and b over the Vindhyan terrain. The sites were chosen so that the subsurface should not suffer any lateral inhomogeneity. Both the curves for Schlumberger as well as axial pole–dipole (MNB) arrays show good match with each other. The interpreted results obtained for these combined arrangements are shown in Table 1. Depth of basement obtained from Schlumberger and axial

pole–dipole arrays in sounding no. KB-37 is 3.43 and 3.4 m; in KB-38, 10.65 and 10.6; in GS-2, 23.5 and 23.9 m, and in GS-3, 68.4 and 67.7 m respectively. Hence the above exercise confirms that results obtained from Schlumberger and axial pole–dipole configurations over the same ground are the same.

However, in the presence of near-surface inhomogeneities, the Schlumberger and pole–dipole curves show little difference in their nature. In the case of the Schlumberger array, the effect of lateral inhomogeneity below the entire spread is averaged out, whereas in the case of axial pole–dipole array the actual inhomogeneity present below the moving current electrode path is reflected well<sup>12</sup>. Thus the axial pole–dipole curve is more sensitive to the near-surface inhomogeneity in case the anomalous body is present at the side of the moving current electrode. This effect can be clearly seen in the Figure 5a and b. These soundings (SPD-1 and SPD-2) have been done over granitic terrain, which has been traversed by dolerite dykes trending in E–W direction. In sounding no. SPD-2, a dyke is towards the active electrode-A (Figure 5a). The apparent resistivity curves of Schlumberger and axial pole–dipole (AMN) begin rising from the starting point (i.e. half current electrode separation  $a/2 = 1.5$  m) up to  $a/2 = 4$  m and then start lowering (AMN curve up to  $a/2 = 12$  m and Schlumberger curve up to  $a/2 = 8$  m); fur-

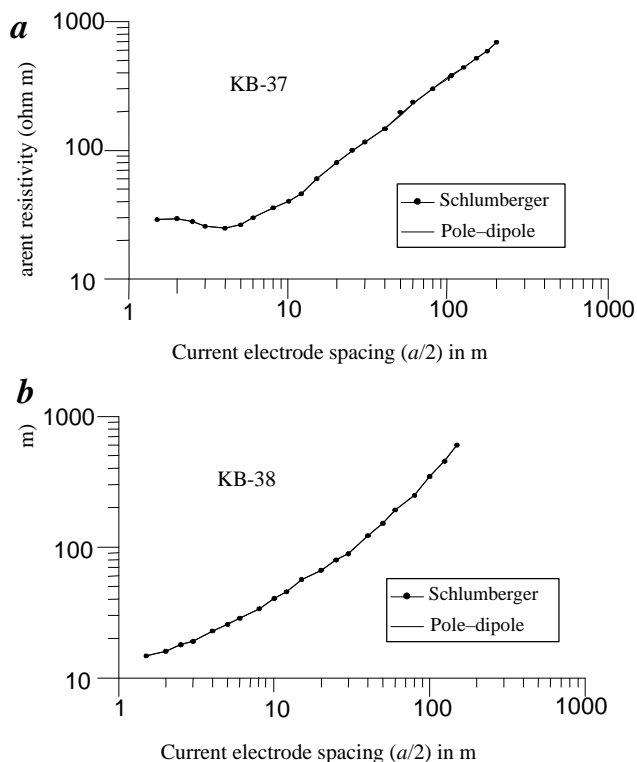


Figure 3a and b. Resistivity curves by Schlumberger and axial pole–dipole configurations in granitic terrain, Kolar district, Karnataka.

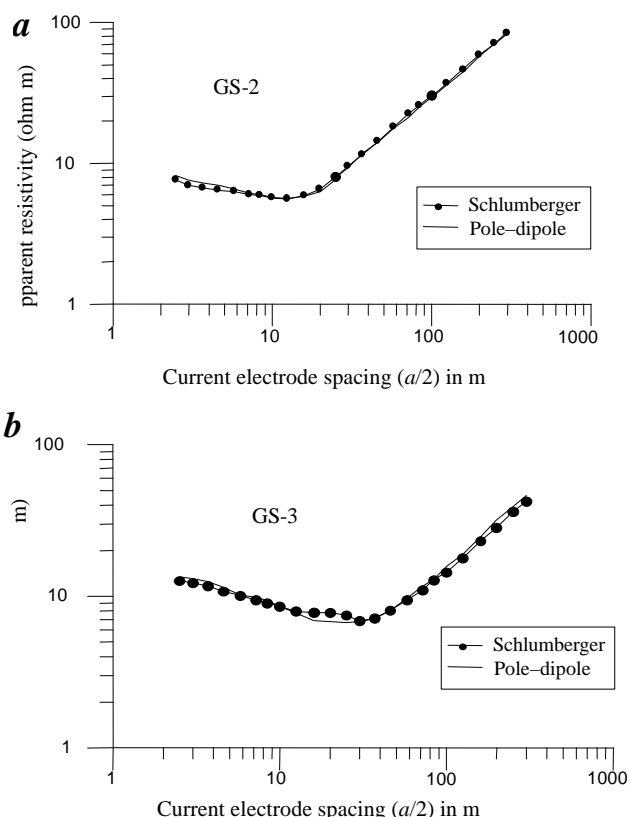


Figure 4a and b. Resistivity curves by Schlumberger and axial pole–dipole configurations in sedimentary terrain, Mirzapur, UP.

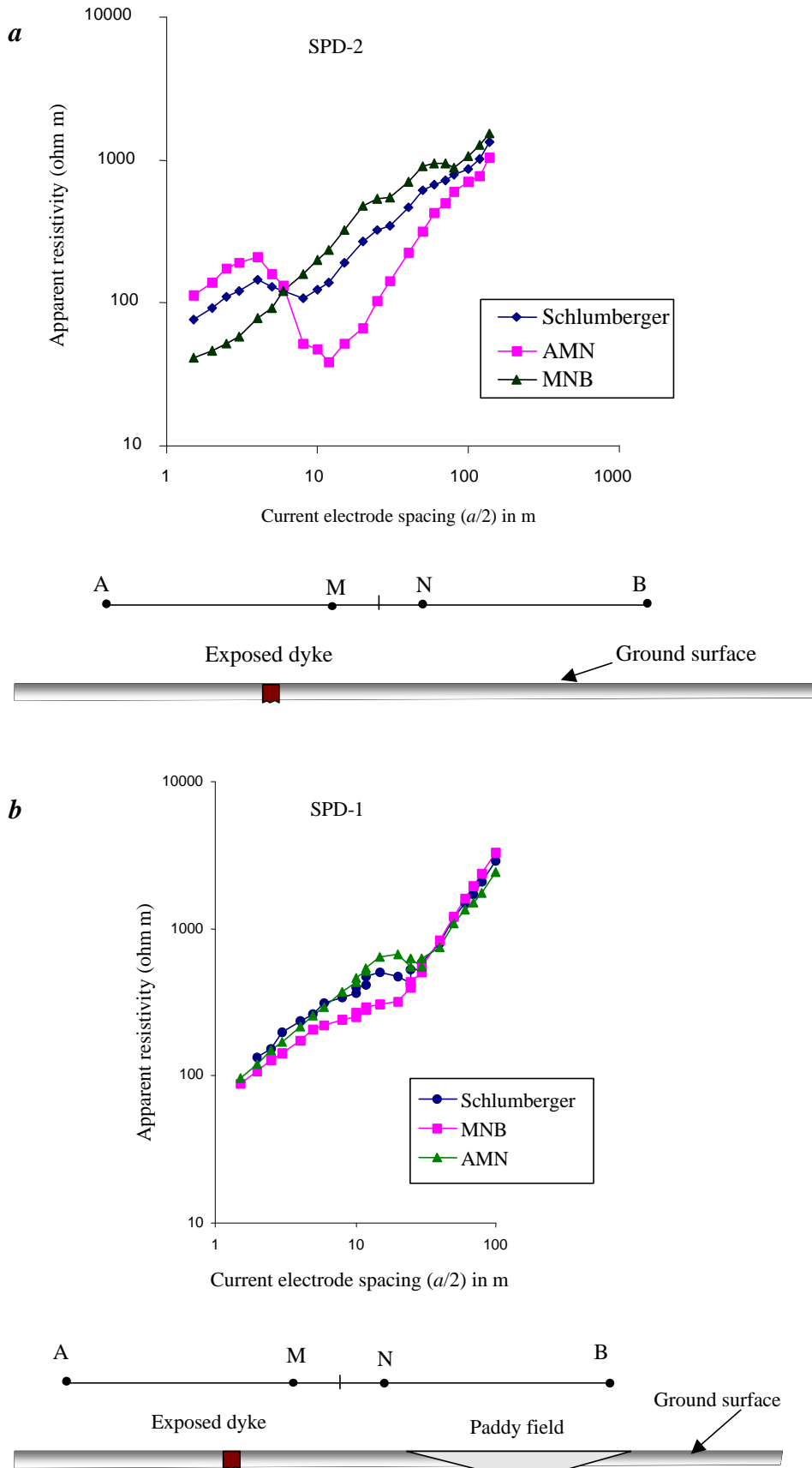


Figure 5. Resistivity curves by Schlumberger and axial pole-dipole configurations across (a) dyke and (b) dyke and paddy field.

**Table 1.** Interpreted layer parameters from Schlumberger and axial pole–dipole arrays

Sounding no.	Schlumberger configuration			Axial pole–dipole configuration			
	Layer no.	Resistivity (ohm m)	Thickness (m)	Total thickness (m)	Resistivity (ohm m)	Thickness (m)	Total thickness (m)
KB-37	1	30.24	1.86	3.43	31.3	1.9	3.4
	2	7.46	1.57		8.0	1.5	
	3	7602.23	–		8876.3	–	
KB-38	1	14.16	2.0	10.65	13.9	1.9	10.6
	2	37.24	8.65		48.9	8.7	
	3	10066.22	–		11494.2	–	
GS-2	1	7.0	3.5	23.50	7.8	3.3	23.9
	2	3.5	8.0		3.9	6.6	
	3	25.2	12		28.2	14.0	
	4	9999	–		9999	–	
GS-3	1	14.1	2.5	68.40	14.5	2.6	67.7
	2	6.5	31.2		6.4	30.3	
	3	20.7	34.7		20.8	34.8	
	4	10012.4	–		110001.5	–	

ther  $a/2$  these values keep on increasing, whereas the apparent resistivity values for axial pole–dipole (MNB) is continuously increasing from 51.7 to 1519.8 ohm m.

In sounding no. SPD-1, a dyke striking across the layout direction, lies approximately 20 m away from the centre of the configuration towards the active electrode-A and a paddy field approximately 25 m from the centre of the configuration towards the active current electrode-B. The AMN is the axial pole–dipole array, where the active electrode is moving towards the dyke and MNB towards the paddy field. The lows in Schlumberger, AMN and MNB curves are not similar (Figure 5 b). A possible cause for this dissimilar low in AMN is due to the dyke, while the low in MNB curve may be due to the paddy field, where relatively thick weathering is expected. The Schlumberger curve, which is affected due to both the dyke as well as the paddy field, is little different from both the curves, viz. AMN and MNB.

Thus the resistivity low obtained by Schlumberger and axial pole–dipole (AMN) curves but no deviation in axial pole–dipole (MNB) curve can be attributed to lateral inhomogeneity (i.e. the dyke). This resistivity low depends upon the position and size of the anomalous body with respect to the moving current electrode. These types of curves could mislead in recommendation of a site for drilling. In case all three curves exhibit low resistivity at the same  $a/2$ , then anomaly may be attributed to sub-surface strata. If the aquifer resistivity and its thickness are suitable for that particular environment, the location can be recommended for drilling.

Thus it can be understood that the combined approach of Schlumberger and axial pole–dipole configurations will help in locating successful sites for drilling in hard-rock areas. The axial pole–dipole array can be used as a

substitute for the Schlumberger configuration, which yields the same result. The vertical electrical sounding by axial pole–dipole array can be carried out even at places where the Schlumberger spread could not be laid due to lack of space on any one side of the sounding point.

The combined set-up of axial pole–dipole and Schlumberger arrays is an appropriate tool in hard-rock areas infested with near-surface inhomogeneities. These arrays can be carried out on the same traverse simultaneously. The comparative study of these curves is helpful in identifying the effect of lateral inhomogeneities in the VES curves. Thus the combination of these arrays can be helpful in locating successful sites for drilling of borewells in laterally inhomogeneous areas.

The axial pole–dipole array can be used as the substitute for the Schlumberger array for groundwater exploration, which yields the same result.

1. Sankaran, S., Vipul Nagar, Subash Chandra and Gopalakrishnan, N., Groundwater exploration in hard rock areas. Post-Conference Proceedings of IGC 2002, pp. 209–216.
2. Van Nostrand, R. E. and Cook, K. L., Interpretation of resistivity data. USGS Professional Paper 499, Washington, 1960.
3. Rakesh Kumar and Chowdary, M. V. R., Effect of vertical contact on Wenner resistivity soundings. *Geophys. Prospect.*, 1977, **25**, 471–480.
4. Zohdy, A. A. R., Eaton, G. P. and Mabey, D. R., Application of surface geophysics to groundwater investigations. USGS, Washington, 1974.
5. Ballukaraya, P. N., Sharma, K. K., Reddi, B. R. and Jagatheesan, M. S., Identification of lateral inhomogeneities from VES curves. *J. Assoc. Explor. Geophys.*, 1988, **10**, 171–183.
6. Keller, G. V. and Frischknecht, F. C., *Electrical Methods in Geophysical Prospecting*, Pergamon, New York, 1966.
7. Frohlich, R. K., The influence of lateral inhomogeneities on the dipole methods. *Geophys. Prospect.*, 1968, **XVI**, 314–325.

8. Ermokhin, K. M., Tsokas, G. N., Tsourlos, P. and Glasunov, V. V., Calculation of the azimuthal inhomogeneity ratio response of 3D structures using an analytical forward modelling scheme. *Balkan Geophys. Soc.*, 1998, **1**, 53–59.
9. Jain, S. C. *et al.*, Evolution of cost-effective and sustainable management scheme of water resources in Bairasagara watershed, Kolar district, Karnataka. NGRI Technical Report No. NGRI-2003-GW-391, p. 46.
10. Subash Chandra, Exploration of groundwater bearing zones in the hard rock area of Bahuti, District Mirzapur (UP), M Sc (Tech) dissertation, 2000, p. 66.
11. Koefoed, O., *Geosounding Principles 1. Resistivity Sounding Measurements*, Elsevier Scientific Company, Amsterdam, 1979.
12. Yadav, G. S., Pole-dipole resistivity sounding technique for shallow investigations in hard rock areas. *PAGEOPH*, 1988, **127**, 63–71.

ACKNOWLEDGEMENTS. We are grateful to the Director, NGRI, Hyderabad for permission to publish this communication. The fieldwork was carried out under a DST-funded project. We also thank to Shri S. C. Jain for useful discussions and suggestions in preparing this manuscript and Mr M. R. K. Sarma who helped in carrying out the fieldwork. Dr G. S. Yadav is acknowledged for his valuable suggestions and discussions during the fieldwork at Mirzapur, UP.

Received 22 July 2003; revised accepted 22 January 2004

## Estimates of plate velocity and crustal deformation in the Indian subcontinent using GPS geodesy

Sridevi Jade

CSIR Centre for Mathematical Modelling and Computer Simulation, Bangalore 560 037, India

GPS studies have been carried out by CSIR Centre for Mathematical Modelling and Computer Simulation (C-MMACS), Bangalore in the Indian subcontinent since 1994 to determine displacement and strain accumulation in the region over the past few years. This communication integrates the results obtained over the years in different regions of the Indian subcontinent using GPS geodesy to get an overall picture of deformation and related interpretations and discussions. The regions broadly covered by C-MMACS are the southern Indian peninsula, Ladakh, Garhwal, Kumaun, Darjeeling, Sikkim, Gujarat, Andamans and Shillong. GPS-derived velocity vectors of about 50 sites are given in the ITRF 97 (International Terrestrial Reference Frame), Indian reference frame and relative to IISc IGS station. Notable conclusions from the above study are as follows: Southern peninsular India moves as a rigid plate with the velocity of Indian plate. Convergence of 10–20 mm/yr occurs in the

**2500 km stretch of the Himalayan arc from Kashmir to Arunachal and the convergence rates vary from west to east. Extension between the Himalayan GPS sites and Lhasa (southern Tibet) site is consistent with the east-west extension of the Tibetan Plateau.**

THE Indian subcontinent is one of the most earthquake-prone areas of the world. Several major earthquakes<sup>1</sup> have occurred at the plate interiors and boundaries in this subcontinent during the last three decades, causing massive losses (Koyna, 1967; Badhrachalam, 1969; Broach, 1970; Udaypur, 1988; Uttarkashi, 1991; Latur, 1993; Jabalpur, 1997; Chamoli, 1999; Bhuj, 2001). Earthquakes in India are mainly caused due to release of elastic strain energy created and replenished by persistent collision of the Indian plate with the Eurasian plate. Though the tectonics of the Indian subcontinent is dynamic and complex, evolution of precise GPS geodesy since 1990 makes it possible to understand the dynamics involved and also the measurement of strain accumulation in the Indian plate. One of the primary objectives of the CSIR Centre for Mathematical Modelling and Computer Simulation (C-MMACS), Bangalore is to generate an insightful understanding of the deformation mechanism in the Indian subcontinent, which is the major cause of earthquakes. This can be achieved using GPS to measure and understand deformation mechanism related to stresses at all scales. This would result in better understanding of physical processes of earthquake phenomena. The geo-tectonics of the Himalayas, Kachchh and south Indian shield, which were covered by a dense network of GPS stations, is discussed briefly.

The Himalayas, Karakoram and Tibetan plateau, which together span a wide deformation zone of 2500 km, are a result of Indo-Eurasian collision. The southern limit of this zone<sup>2</sup> of compressive intercontinental deformation is marked by a smooth circular arc of the Himalayan fold and thrust belt that rises abruptly over the under thrusting. Both the geological structure and active tectonics<sup>3</sup> along the 2500 km stretch of the Himalayan arc from Kashmir to Arunachal, are of significant importance due to continuous seismic activities in this region. The Kachchh region of western India<sup>4</sup> is an excellent example of a tectonically controlled landscape comprising an assemblage of various geomorphic features. This region has a unique history of continued tectonism (Kachchh, 1819; Anjar, 1956; Bhuj, 2001), which is a reflection of movements along major faults; Kathiawar fault, Nagar Parkar fault, Allah Bund fault and Kachchh mainland fault. Earthquakes in the Indian peninsular shield fall in the category of Stable Continental Region Events. Monitoring of these events is of paramount importance, as many tectogenic faults may be responding to the present crustal deformation process. Continental crust of southern India<sup>5</sup> exhibits unique characteristics whose geophysical signatures differ markedly from those of its counterparts in other parts

e-mail: sridevi@cmmacs.ernet.in